Corrected Aeroelastic Flutter and Divergence Analysis of Swept Wings with Stiffness Cross-Coupling

By John R. Cipolla, Aerospace and Mechanical Engineer
Work performed from June 1990 to August 1990, while working in the CFD Section,
Aerodynamics Branch, Air Force Armament Laboratory (AFAL), Eglin AFB, Florida

Abstract

The 1986 AIAA paper *Control of Aeroelastic Instability Through Stiffness Cross-Coupling* presented a derivation of aeroelastic flutter analysis for wings with stiffness cross-coupling, including forward-swept configurations. In applying the AIAA Journal of Aircraft formulation to practical design work, we identified five typographical errors that can lead to incorrect flutter and divergence velocities. Our paper re-derived the entire set of aeroelastic cross-coupling equations including the mass matrix, stiffness matrix, aerodynamic matrix, and vibration equations of motion, then identified and corrected the affected relationships. The corrected results express flutter velocity and divergence velocity as functions of the stiffness cross-coupling parameter and the torsional-to-bending stiffness ratio. Because the formulation applies to unswept, forward-swept, and rear-swept wings and fins in subsonic flow, these corrections are important for practical aeroelastic design and analysis. The corrected formulation is then compared with results produced from the unmodified published equations to show how the errors affect practical forward-swept, rear-swept, and unswept lifting-surface analyses for subsonic speeds.

Nomenclature

y_{cp} = Center-of-pressure location measured along y axis from root
e = Line of aerodynamic centers located at the ¼ chord point from the y-axis
Λ = Sweep angle y-axis makes with respect to the freestream velocity
x_α = Distance of centers of mass from the reference axis, y
c = Chord length
ℓ = Wingspan along reference axis, y
AR = Wing aspect ratio (ℓ/c)
CL_α = Wing lift slope
r_α = Radius of gyration
ω_θ = Torsional spring constant
ω_ϕ = Bending spring constant
ψ = Stiffness cross-coupling parameter
R = Ratio of torsional to bending stiffness parameter
μ = Ratio of wing mass to air mass around the wing
V_{ref} = Non-dimensional flutter and divergence speed
V_F = Flutter velocity
V_D = Divergence velocity

Copyright © 2026 John Cipolla/AeroCFD.com

Introduction

This paper presents a mathematical model[1] of a cantilever wing and its structural stiffness matrix to show how bending-torsion stiffness cross-coupling affects flutter and divergence. By layering advanced composite materials at specific angles, the resulting anisotropic structural forces cause upward bending from aerodynamic forces to automatically twist the leading edge downward, shedding lift and stabilizing the wing against flutter and divergence. The resulting computational method allows an engineer to evaluate how changes in fiber directional stiffness orientation affect flutter and divergence velocities of forward-swept, rear-swept, and unswept wings and fins.

This paper provides a corrected and independently documented computational path for aeroelastic stability analysis with bending-torsion stiffness cross-coupling. Rather than treating the published errors as isolated typographical corrections, this work re-derives the affected mass, stiffness, aerodynamic, and equation-of-motion relationships, identifies where the errors enter the flutter and divergence solution, and compares corrected results with results obtained from the original published equations. The corrected formulation clarifies how stiffness cross-coupling and torsional-to-bending stiffness ratio influence predicted stability boundaries, making the analysis more reliable for swept-wing and fin design studies in subsonic flow. Specifically, the errors identified in the paper *Control of Aeroelastic Instability Through Stiffness Cross-Coupling*[1] are in equations 14, 16, 22, 23 and 25. These errors are summarized in Table-1.

Table 1: Summarizes the five corrected relationships and explains how each correction affects the aeroelastic analysis

Original equation	Error type	Corrected issue	Practical effect
Equation 14	Sign error	Corrects the sign in the aerodynamic equations of motion that combine stiffness and aerodynamic terms.	Restores the proper balance between structural stiffness and aerodynamic loading in the stability formulation.
Equation 16	Reference-frequency expression	Corrects the reference frequency used to normalize flutter and divergence velocity.	Affects nondimensional velocity scaling and comparison of computed stability boundaries.
Equation 22	Coefficient d error	Corrects the coefficient used in the flutter and divergence velocity solution.	Changes the computed stability boundaries as stiffness cross-coupling is varied.
Equation 23	Lift-coefficient relation	Corrects the aerodynamic lift coefficient relationship used to form the aerodynamic matrix.	Improves consistency of the aerodynamic loading terms used in the aeroelastic equations.
Equation 25	Coefficient g error	Corrects the coefficient used with coefficient d in computing flutter and divergence velocity.	Alters the final predicted flutter and divergence velocities and shifts the plotted stability curves.

First, Equation (14) in the Journal of Aircraft paper contains an incorrect positive sign in the aerodynamic equations of motion, which include stiffness and aerodynamic terms. The incorrect relationship is shown as Equation (1), and the corrected relationship is shown as Equation (2). For simplicity, the mass and stiffness matrices are reduced to M and K terms to save space.

$$\begin{bmatrix} M_{11}+K_{11} & M_{12}+K_{12} \\ M_{12}+K_{12} & M_{22}+K_{22} \end{bmatrix}\begin{pmatrix}\boldsymbol{\theta}\\ \boldsymbol{\varphi}\end{pmatrix} + \frac{1}{2}\left(\frac{(\boldsymbol{V}\cos\Lambda)^2\, CL_\alpha}{\pi\,\mu\, \boldsymbol{r_\alpha}^2}\right)\begin{bmatrix} -\boldsymbol{e} & \boldsymbol{e}\ \tan\Lambda \\ +\boldsymbol{y}\ \boldsymbol{AR} & \mathbf{y}\ \mathbf{AR}\ \tan\Lambda \end{bmatrix}\begin{pmatrix}\boldsymbol{\theta}\\ \boldsymbol{\varphi}\end{pmatrix} = \begin{pmatrix}0\\0\end{pmatrix} \qquad (1)$$

$$\begin{bmatrix} M_{11}+K_{11} & M_{12}+K_{12} \\ M_{12}+K_{12} & M_{22}+K_{22} \end{bmatrix}\begin{pmatrix}\boldsymbol{\theta}\\ \boldsymbol{\varphi}\end{pmatrix} + \frac{1}{2}\left(\frac{(\boldsymbol{V}\cos\Lambda)^2\, CL_\alpha}{\pi\,\mu\, \boldsymbol{r_\alpha}^2}\right)\begin{bmatrix} -\boldsymbol{e} & \boldsymbol{e}\ \tan\Lambda \\ -\boldsymbol{y}\ \boldsymbol{AR} & \mathbf{y}\ \mathbf{AR}\ \tan\Lambda \end{bmatrix}\begin{pmatrix}\boldsymbol{\theta}\\ \boldsymbol{\varphi}\end{pmatrix} = \begin{pmatrix}0\\0\end{pmatrix} \qquad (2)$$

Second, the incorrect equation for reference frequency[2], identified as Equation (16) in the Journal of Aircraft paper, is presented on the **left** and the corrected equation on the **right**, below.

$$\omega_p{}^2 = K_{11}M_{11} \qquad\qquad \omega_p{}^2 = \frac{K_{11}}{M_{11}} \tag{3}$$

Third, the incorrect equation for coefficient, d required to compute flutter velocity[2], and divergence velocity[2], identified as Equation (22) in the Journal of Aircraft paper, is presented as Equation (4), and the corrected relationship is shown as Equation (5).

$$\mathrm{d} = -\varepsilon\, AR \left[\mathbf{y}\ \tan\Lambda \frac{-AR\,\boldsymbol{e}}{3\,\mathbf{r}^2{}_\alpha} + \frac{\mathbf{x}_\alpha}{2\,\mathbf{r}^2{}_\alpha}\ (\boldsymbol{e}\ \tan\Lambda - \boldsymbol{y}\, AR\,)\right] \tag{4}$$

$$\mathrm{d} = -\varepsilon\, AR \left[\mathbf{y}\ \tan\Lambda - \frac{AR\,\boldsymbol{e}}{3\,\mathbf{r}^2{}_\alpha} + \frac{\mathbf{x}_\alpha}{2\,\mathbf{r}^2{}_\alpha}\ (\boldsymbol{e}\ \tan\Lambda - \boldsymbol{y}\, AR\,)\right] \tag{5}$$

Fourth, the equation for lift coefficient[4,5,6], identified as Equation (23) in the Journal of Aircraft paper, is presented on the **left** and the corrected equation on the **right**, below.

$$\xi = \frac{CL_\alpha}{2\pi^2\,\mu\, r_\alpha{}^2} \qquad\qquad \xi = \frac{CL_\alpha}{2\pi\,\mu\, r_\alpha{}^2} \tag{6}$$

Fifth, the incorrect equation for coefficient, g required to compute flutter velocity, and divergence velocity, identified as Equation (25) in the Journal of Aircraft paper, is presented as Equation (7), and the corrected relationships are shown in the equation 8-1 and 8-2, below.

$$g = \varepsilon\left[-e + R\, y\, AR\ \tan\Lambda + \psi\sqrt{R}(e\ \tan\Lambda - y\, AR)\right] \tag{7}$$

$$g = \frac{\varepsilon}{R}\left[-e + R\, y\, AR\ \tan\Lambda + \psi\sqrt{R}(e\ \tan\Lambda - y\, AR)\right] \tag{8^1}$$

$$g = \varepsilon\left[-\frac{e}{R} + y\, AR\ \tan\Lambda + \frac{\psi}{\sqrt{R}}(e\ \tan\Lambda - y\, AR)\right] \tag{8^2}$$

Aeroelastic Model Development

The following section presents the full derivation of the idealized aeroelastic model used in the referenced 1986 Journal of Aircraft paper. The original work was intended for parametric studies of forward-swept and rear-swept wings and fins. The idealized model equations presented in Figures 9 through 14 are suitable for studying flutter velocity and divergence velocity for semirigid wings and fins swept at an angle to the airstream and attached to a fixed wall point in an airstream of velocity, V. In this model, flutter and divergence are mechanical instabilities caused by aeroelastic interaction between the bending and torsional vibration modes of a wing idealized as a cantilever beam. The system is represented as a two-degree-of-freedom swept lifting surface with uniform spanwise mass distribution and a rigid root attachment. The reference axis of the lifting surface is defined as the y-axis and is attached at a single point on the root of the cantilever beam, as shown in Figure 1. Displacement about the x and z axes during sinusoidal vibration is shown in Figures 1 and 2, where the reference axis y is swept at an angle relative to the freestream velocity. The line of aerodynamic centers, e, is located at the quarter-chord point from the y-axis for subsonic flow. The line of centers of mass is offset from the reference axis y by the distance shown and is positive when the centers of mass are behind the reference axis. The chord c and span ℓ define the lifting-surface planform and aspect ratio.

Figure 2 defines the stiffness axes oriented at angles γ and γ + 90 degrees with respect to the reference axis y. The torsion spring constant is associated with twisting about the principal stiffness axis at angle γ relative to the reference axis. The bending spring constant is associated with rotation about the principal stiffness axis normal to that direction. Together, the torsion and bending stiffness parameters simulate the elastic response of the airfoil at the wall attachment

point. Where, K_θ is associated with twisting around the principal stiffness axis[2] at angle, γ with respect to the reference axis, y and the bending spring constant, K_ϕ is associated with twisting around the principal stiffness axis normal to the y-axis.

The attached six pages of derivations begin with the aerodynamic loads[5,6] that act perpendicular to the reference axis, y, and derive the matrix of aerodynamic moments[8] around the span and chord axes at the attachment point. The cross-coupling derivation analysis is presented in Figures 9 through 14. The first equation in the six-page derivation is the aerodynamic matrix due to aerodynamic loading and appears below as Equation (9). The remaining results for stiffness cross-coupling flutter and divergence are presented in Figures 9 through 14.

$$\begin{Bmatrix} M_\theta \\ M_\phi \end{Bmatrix} = qSCL_\alpha \cos^2\Lambda \begin{bmatrix} e & -e\tan\Lambda \\ y_{cp} & -y_{cp}\tan\Lambda \end{bmatrix} \begin{Bmatrix} \theta \\ \phi \end{Bmatrix} \tag{9}$$

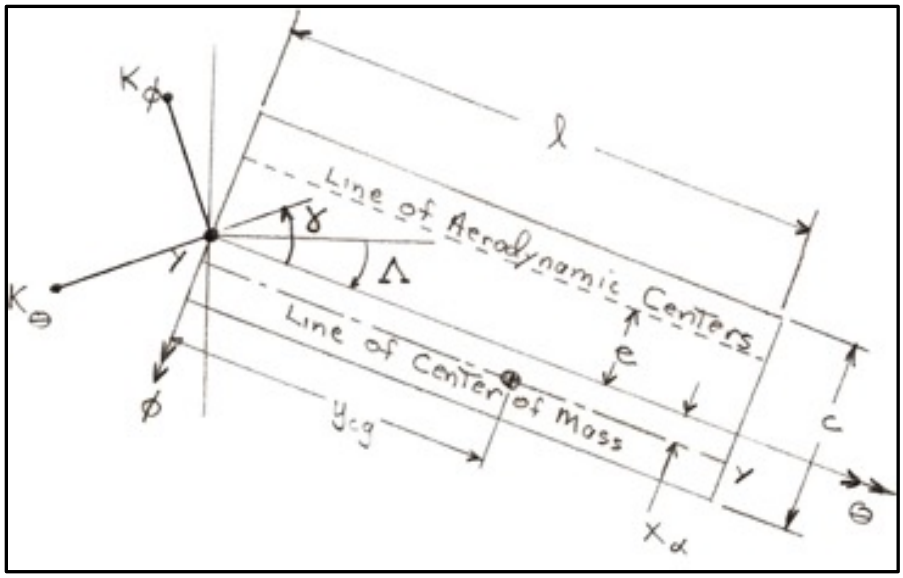

Figure 1. Idealized swept lifting-surface model showing how torsional and bending rotations are defined about the reference-axis attachment point.

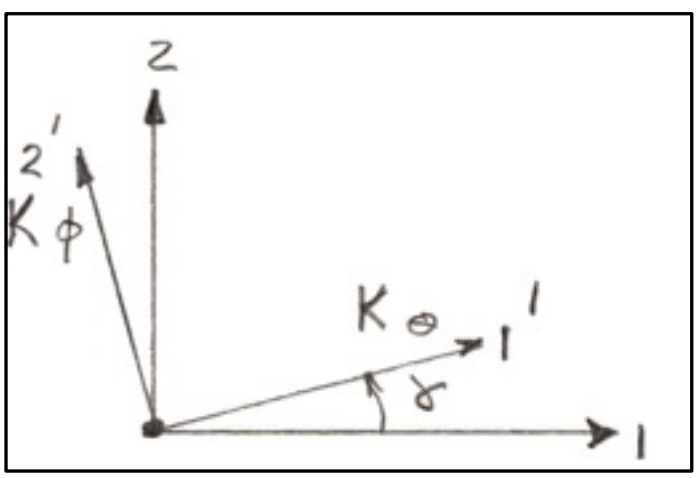

Figure 2. Principal stiffness-axis orientation used to introduce bending-torsion cross-coupling into the swept-wing structural model.

Computational Flow Diagram

$$\mathrm{a} = \frac{\mathrm{AR}^2}{3\, r^2{}_\alpha}\left[\frac{\mathbf{r}^2{}_0 + \frac{1}{4}\mathbf{x}^2{}_\alpha}{\mathbf{r}^2{}_\alpha}\right] \tag{10}$$

$$\mathrm{d} = -\varepsilon\, AR\left[\mathbf{y}\,\tan\Lambda - \frac{AR\,\boldsymbol{e}}{3\,\mathbf{r}^2{}_\alpha} + \frac{\mathbf{x}_\alpha}{2\,\mathbf{r}^2{}_\alpha}\,(\boldsymbol{e}\,\tan\Lambda - \boldsymbol{y}\,AR\,)\right] \tag{11}$$

$$\varepsilon = \frac{C_{L\alpha}}{2\pi\,\mu\,\mathbf{r}^2{}_\alpha} \qquad \mu = \frac{2\,m}{\pi\,\rho\,\frac{c}{2}} \qquad V_{ref} = c\,\omega_\theta\sqrt{\mu} \tag{12}$$

$$R = 3.5, 1.0, 0.30 \tag{13}$$

$$\mathrm{b} = -\frac{1}{R}\left[1 + \frac{R\,AR^2}{3\,\mathbf{r}^2{}_\alpha} - \frac{\mathbf{x}_\alpha\,AR\,\sqrt{R}\,\psi}{\mathbf{r}^2{}_\alpha}\right] \tag{14}$$

$$g = \varepsilon\left[-\frac{e}{R} + y\,AR\,\tan\Lambda + \frac{\psi}{\sqrt{R}}(e\,\tan\Lambda - y\,AR)\right] \tag{15}$$

$$f = \frac{1-\psi^2}{R} \qquad y = \frac{y_{cp}}{\ell} \tag{16}$$

$$V_F{}^2 = \frac{-(bd-2ag)\pm 2\left[a\left(-bdg+ag^2+d^2f\right)\right]^{1/2}}{d^2\cos^2\Lambda} \tag{17}$$

$$V_D{}^2 = -\frac{f}{g} \tag{18}$$

---------- Plot ----------

$$V_F = \frac{V_F}{V_{ref}}\ \ and\ \ V_D = \frac{V_D}{V_{ref}} \qquad versus \qquad \psi\ and\ R \tag{19}$$

Loop to Equation 14 to increment stiffness cross-coupling, ψ from -1 to 1
Loop to Equation 13 for each ratio of torsional to bending stiffness, R=3.5, 1.0 and 0.30

$$\psi = \frac{-K_{12}}{\sqrt{K_{11}\,K_{22}}}\quad(-1 < \psi < 1) \qquad R = \frac{K_{11}}{K_{22}} \tag{20}$$

Figure 3. Computational flow diagram used to calculate nondimensional flutter and divergence velocities while sweeping stiffness cross-coupling and torsional-to-bending stiffness ratio.

Computational Method and Journal of Aircraft Results Compared

Figure 4 presents the corrected Mathcad results for flutter and divergence velocity as functions of stiffness cross-coupling and torsional-to-bending stiffness ratio for a 15-degree sweptback wing. The example-wing parameters used to compute the reference velocity are listed in Table 2, and the computational sequence follows the flow diagram in Figure 3. For each value of torsional-to-bending stiffness ratio, R the stiffness cross-coupling parameter, ψ is swept from −1 to 1. Solid curves represent flutter velocity, and dotted curves represent divergence velocity. The **red** curves correspond to R = 3.5, the **black** curves correspond to R = 1.0, and the **blue** curves correspond to R = 0.3. As expected, the corrected Mathcad results show a dependence of flutter and divergence velocity on stiffness cross-coupling as a function of torsional-to-bending stiffness ratio. Also, these results agree with the original paper that each flutter velocity intersects the corresponding

divergence velocity for the same torsional-to-bending stiffness ratio. In addition, the overall velocity range is consistent with the range used in the AIAA Journal of Aircraft paper.

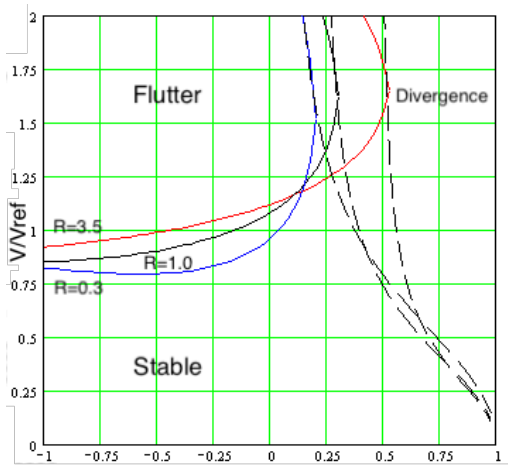

Figure 4. Corrected Mathcad results predict flutter and divergence boundaries that vary systematically with stiffness cross-coupling; the divergence curves intersect the corresponding flutter curves for the same torsional-to-bending stiffness ratio. Flutter and divergence velocity curves exactly match the Journal of Aircraft results in that paper's Figure 4 (Figure 6 below) for sweep, $\Lambda = 15\ degrees$

Please notice the corrected formulations for equations 14, 16, 22, 23 and 25 used in the Mathcad analysis to predict flutter and divergence velocity exactly match results from the AIAA Journal of Aircraft paper presented in Figure 6 where the results of the paper are labeled as Fig. 4.

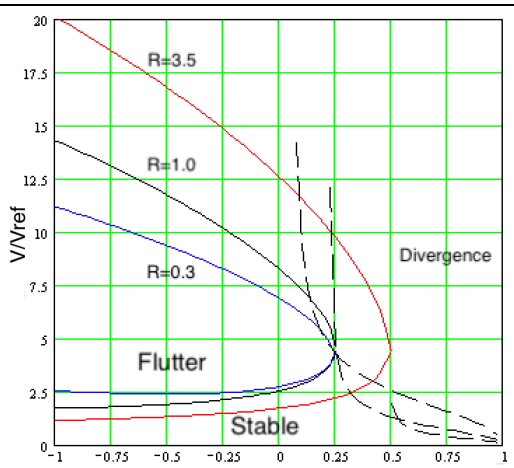

Figure 5. Using the **original** Journal of Aircraft equations for a sweptback wing in Mathcad shifts the computed flutter and divergence velocity curves, demonstrating the errors for $\Lambda = 15\ degrees$

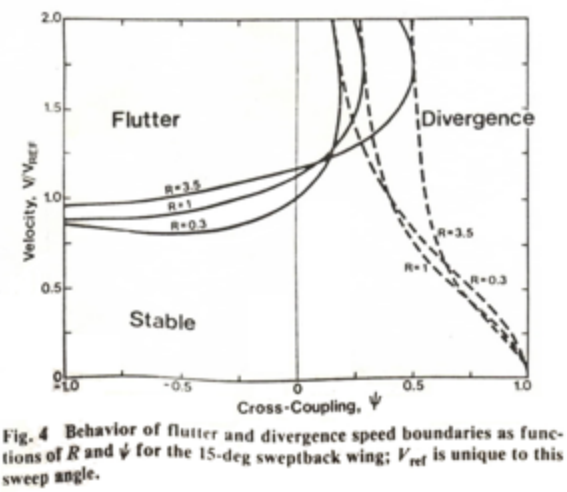

Figure 6. Original swept wing plot from Journal of Aircraft, under fair use for comparative analysis when evaluating the curve shifts produced by the incorrect formulation.

Figure 5 isolates the effect of the original AIAA Journal of Aircraft equations by applying the computational method from Figure 3 without the corrections identified in this paper. Comparing Figure 5 with the published baseline in Figure 6 shows that the five typographical errors affect more than isolated numerical values; they shift the relative positions and magnitude of the flutter and divergence stability curves. The comparison therefore supports the central conclusion of this paper: the corrected equations are necessary to obtain a consistent relationship between stiffness cross-coupling, torsional-to-bending stiffness ratio, and predicted flutter or divergence onset. For practical swept-wing and fin design, this distinction matters because an incorrect curve shift could lead to either excessive conservatism or an unconservative prediction of aeroelastic stability.

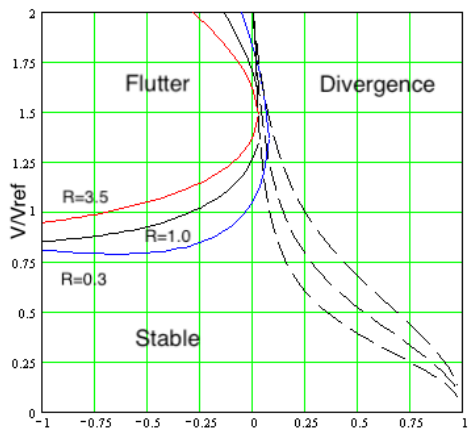

Figure 7. Mathcad spreadsheet results for an unswept wing using the corrected equations from Table 1, the flutter and divergence stability curves exactly match the AIAA Journal of Aircraft results in that paper's Figure 3 for sweep, $\Lambda = 0.0\ degrees$.

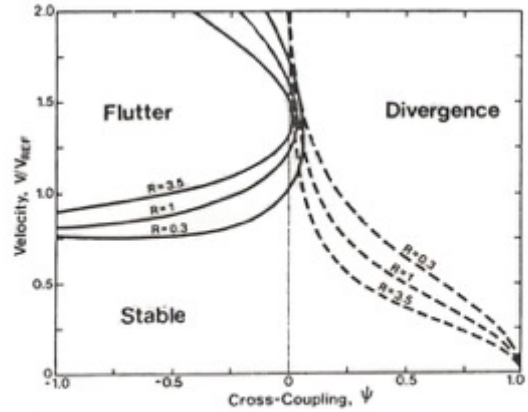

Fig. 3 Flutter and divergence speed boundaries as functions of R and ψ for an unswept wing (Table 1). Dashed line, divergence speed; solid lines, flutter.

Figure 8. Original unswept wing plot shown as Figure 3 in the Journal of Aircraft used under fair use for comparative analysis for evaluating the corrected formulation. Notice the results from Figure 3 match the Mathcad results.

Finally, flutter velocity and divergence velocity computed by the Mathcad analysis are plotted in Figure 7 for a zero-degree sweptback wing and plotted side by side with results from the Journal of Aircraft paper for the same sweep angle in Figure 8. The flutter velocity and divergence velocity results from the Journal of Aircraft paper and Mathcad analysis match exactly. These results indicate the errors in the Journal of Aircraft paper are isolated to where lift coefficient, ε and sweep angle, Λ appears in the aeroelastic equations, i.e. Equation 22, 23 and 25 in the original paper. These equations are the source of the errors in the paper because these equations are used to compute flutter velocity and divergence velocity in Equation 17 and 18 in the computational flow diagram. Then, although not presented here, if the original Journal of Aircraft equations are used in the Mathcad analysis, the curves do not appear in the velocity range of the plot for the zero-degree sweptback wing. This is further evidence the errors in the original AIAA paper have been successfully corrected.

Table 2: Describes parameters for example wing

e=0.10	$CL_\alpha = 4.0/rad$
y=0.50	$\mu = 10.0$
$x_\alpha = 0.10$	ℓ/c=AR=4.0
${r_\alpha}^2 = 0.25$	$\Lambda = 0\ and\ 15\ degrees$
$\delta\Lambda = 0.025\ degrees$	R= 3.5, 1.0, 0.30
$\omega_\theta = 1$	c = 1.0
$V_{ref} = c\ \omega_\theta\sqrt{\mu}$	

Summary

This paper re-derived the aeroelastic stiffness cross-coupling formulation to identify and correct five errors in the published equations. The corrected derivation includes the mass matrix, stiffness matrix, aerodynamic matrix, and vibration equation of motion terms needed to compute flutter and divergence velocity. The resulting expressions give flutter velocity and divergence velocity as functions of the stiffness cross-coupling parameter, ψ and the torsional-to-bending stiffness ratio, R, and provide corrected relationships for practical swept and unswept lifting-surface analyses. These results determined that Equation 22, 23 and 25 of the 1986 paper are the source of the errors in the AIAA Journal of Aircraft paper and are typographical while the plots are correct.

History of "Corrected Aeroelastic Flutter and Divergence Analysis of Swept Wings with Stiffness Cross-Coupling" Technical Paper

The following historical note is included to document the origin, interruption, and later completion of this aeroelastic correction effort. Therefore, this paper presents results from an investigation into the errors present in the AIAA Journal of Aircraft paper, *Control of Aeroelastic Instability Through Stiffness Cross-Coupling.* Work was performed from June 1990 to August 1990, while working in the CFD Section, Aerodynamics Branch, Air Force Armament Laboratory (AFAL), Eglin AFB, Florida. Originally, the analyses were performed using a Fortran program on the Eglin Cray-YMP supercomputer using the computational flow diagram displayed in Figure 3. For this paper finally completed decades later, Mathcad has been used to compute flutter velocity and divergence velocity described by the flow diagram.

However, this work was cut short of final AIAA publication because the author, John Cipolla was involved in a reduction in force (RIF) that suddenly terminated the project and his AFAL employment in 1990. However, there were other needs for the author's skills when during the first Gulf war John Cipolla was tasked to perform aircraft flutter compatibility analyses of the Bunker Buster superbomb known as the GBU-28. For this work the author received a United States Air Force performance award for assuring the loads and flutter compatibility of the GBU-28 with the F-111 aircraft. This work was performed at Eglin AFB while employed by the USAF 3246 Test Wing, Office of Aircraft Compatibility, Flutter Section before being laid off in June 1991.

Document History & Context

The math and analytical errors addressed in this paper were originally identified by the author in 1990. This document serves to formally preserve and publish the corrected derivations. This work presents a comprehensive, independent re-derivation and correction of the flutter stiffness cross-coupling wing analysis framework originally published in the Journal of Aircraft (1986). Errors identified in the 1986 analytical framework have been fully resolved herein. Except for two referenced validation figures attributed to the AIAA, the mathematical derivations, text, and numerical plots contained in this document represent the original work of the author and are distributed under a Creative Commons Attribution 4.0 International License (CC BY 4.0).

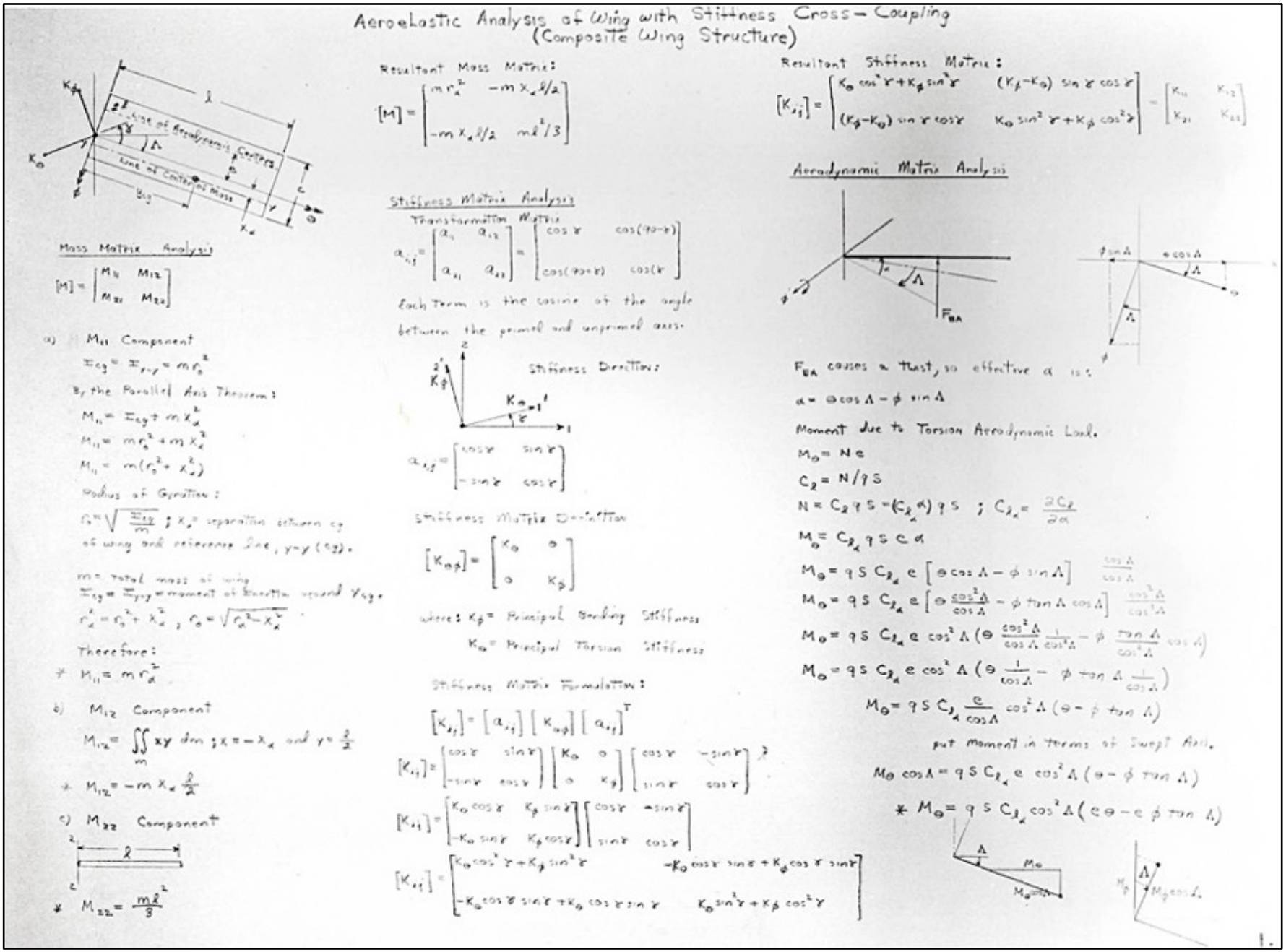

Figure 9. Historical project record documenting the original aeroelastic flutter analysis effort and its connection to the corrected stiffness cross-coupling study.

Moment due to Bending Aerodynamic Load

$$M_\phi = N\, Y_{cp}$$

$$C_L = \frac{N}{qS}$$

$$N = C_L\, q S = (C_{L_\alpha}\, \alpha)\, q S$$

$$M_\phi = C_L\, q S\, Y_{cp}\, \alpha$$

$$M_\phi = q S\, C_{L_\alpha}\, Y_{cp} \left[\theta \cos\Lambda - \phi \sin\Lambda\right] \frac{\cos\Lambda}{\cos\Lambda}$$

$$M_\phi = q S\, C_{L_\alpha}\, Y_{cp} \left[\theta \frac{\cos^2\Lambda}{\cos\Lambda} - \phi \tan\Lambda \cos\Lambda\right] \frac{\cos^2\Lambda}{\cos^2\Lambda}$$

$$M_\phi = q S\, C_{L_\alpha}\, Y_{cp} \cos^2\Lambda \left(\theta \frac{1}{\cos\Lambda} - \phi \tan\Lambda \frac{1}{\cos\Lambda}\right)$$

$$M_\phi = q S\, C_{L_\alpha} \frac{Y_{cp}}{\cos\Lambda} \cos^2\Lambda\, (\theta - \phi \tan\Lambda)$$

put Moment in terms of Swept Axis:

$$M_\phi \cos\Lambda = q S\, C_{L_\alpha}\, Y_{cp} \cos^2\Lambda\, (\theta - \phi \tan\Lambda)$$

$$* \quad M_\phi = q S\, C_{L_\alpha} \cos^2\Lambda\, (Y_{cp}\, \theta - Y_{cp}\, \phi \tan\Lambda)$$

Put into Matrix Form (Matrix Equation)

$$\begin{Bmatrix} M_\theta \\ M_\phi \end{Bmatrix} = q S\, C_{L_\alpha} \cos^2\Lambda \begin{bmatrix} c & -c\tan\Lambda \\ Y_{cp} & -Y_{cp}\tan\Lambda \end{bmatrix} \begin{Bmatrix} \theta \\ \phi \end{Bmatrix}$$

The Aerodynamic Matrix is:

$$[A] = \begin{bmatrix} c & -c\tan\Lambda \\ Y_{cp} & -Y_{cp}\tan\Lambda \end{bmatrix}$$

The Aerodynamic Loads Equation can be expressed as:

$$\begin{Bmatrix} M_\theta \\ M_\phi \end{Bmatrix} = [A_{ij}] \begin{Bmatrix} \theta \\ \phi \end{Bmatrix} .$$

Equation of Motion For Vibration of the airfoil in the presence of an Airstream.

$$\Sigma F = ma$$

$$ma - \Sigma F = 0$$

$$\begin{bmatrix} m r_\alpha^2 & -m x_\alpha l/2 \\ -m x_\alpha l/2 & m l^2/3 \end{bmatrix} \begin{Bmatrix} \ddot\theta \\ \ddot\phi \end{Bmatrix} + \begin{bmatrix} K_\theta \cos^2\gamma + K_\phi \sin^2\gamma & (K_\phi - K_\theta)\sin\gamma\cos\gamma \\ (K_\phi - K_\theta)\sin\gamma\cos\gamma & K_\theta \sin^2\gamma + K_\phi \cos^2\gamma \end{bmatrix} \begin{Bmatrix} \theta \\ \phi \end{Bmatrix} + q S\, C_{L_\alpha} \cos^2\Lambda \begin{bmatrix} -c & c\tan\Lambda \\ -Y_{cp} & Y_{cp}\tan\Lambda \end{bmatrix} \begin{Bmatrix} \theta \\ \phi \end{Bmatrix} = \begin{Bmatrix} 0 \\ 0 \end{Bmatrix}$$

$$\begin{bmatrix} M_{11} & M_{12} \\ M_{21} & M_{22} \end{bmatrix} \begin{Bmatrix} \ddot\theta \\ \ddot\phi \end{Bmatrix} + \begin{bmatrix} K_{11} & K_{12} \\ K_{21} & K_{22} \end{bmatrix} \begin{Bmatrix} \theta \\ \phi \end{Bmatrix} + \begin{bmatrix} A_{11} & A_{12} \\ A_{21} & A_{22} \end{bmatrix} \begin{Bmatrix} \theta \\ \phi \end{Bmatrix} = \begin{Bmatrix} 0 \\ 0 \end{Bmatrix}$$

Assume Harmonic Sinusoidal Motion:

$$\theta = \bar\theta e^{st} \qquad \phi = \bar\phi e^{st} \qquad l/c = AR \qquad \omega_\phi = \sqrt{\frac{K_{11}}{M_{11}}}$$

$$\dot\theta = s\bar\theta e^{st} \qquad \dot\phi = s\bar\phi e^{st} \qquad \psi = \frac{-K_{12}}{\sqrt{K_{11} K_{22}}} \; ; \; R = K_{11}/K_{22}$$

$$\ddot\theta = s^2\bar\theta e^{st} \qquad \ddot\phi = s^2\bar\phi e^{st}$$

$$\begin{bmatrix} M_{11} & M_{12} \\ M_{21} & M_{22} \end{bmatrix} \begin{Bmatrix} s^2\bar\theta e^{st} \\ s^2\bar\phi e^{st} \end{Bmatrix} + \begin{bmatrix} K_{11} & K_{12} \\ K_{21} & K_{22} \end{bmatrix} \begin{Bmatrix} \bar\theta e^{st} \\ \bar\phi e^{st} \end{Bmatrix} + \begin{bmatrix} A_{11} & A_{12} \\ A_{21} & A_{22} \end{bmatrix} \begin{Bmatrix} \bar\theta e^{st} \\ \bar\phi e^{st} \end{Bmatrix} = \begin{Bmatrix} 0 \\ 0 \end{Bmatrix}$$

$$\begin{bmatrix} s^2 M_{11} & s^2 M_{12} \\ s^2 M_{21} & s^2 M_{22} \end{bmatrix} \begin{Bmatrix} \bar\theta \\ \bar\phi \end{Bmatrix} + \begin{bmatrix} K_{11} & K_{12} \\ K_{21} & K_{22} \end{bmatrix} \begin{Bmatrix} \bar\theta \\ \bar\phi \end{Bmatrix} + \begin{bmatrix} A_{11} & A_{12} \\ A_{21} & A_{22} \end{bmatrix} \begin{Bmatrix} \bar\theta \\ \bar\phi \end{Bmatrix} = \begin{Bmatrix} 0 \\ 0 \end{Bmatrix}$$

$$\begin{bmatrix} s^2 M_{11} + K_{11} & s^2 M_{12} + K_{12} \\ s^2 M_{21} + K_{21} & s^2 M_{22} + K_{22} \end{bmatrix} \begin{Bmatrix} \bar\theta \\ \bar\phi \end{Bmatrix} + \begin{bmatrix} A_{11} & A_{12} \\ A_{21} & A_{22} \end{bmatrix} \begin{Bmatrix} \bar\theta \\ \bar\phi \end{Bmatrix} = \begin{Bmatrix} 0 \\ 0 \end{Bmatrix}$$

Substitution Variables For Mass/Stiffness Matrix:

a) $\bar s^2 = \frac{s^2}{\omega_\phi^2} = \frac{s^2}{1} \frac{M_{11}}{K_{11}} \implies \bar s^2 = s^2 \frac{M_{11}}{K_{11}}$: assume $K_{11} = 1$ (Normalized to Torsion)

$$\bar s^2 = s^2 M_{11}$$

b) $\psi = \frac{-K_{12}}{\sqrt{K_{11} K_{22}}}$ and $R = \frac{K_{11}}{K_{22}}$

$$\frac{\psi}{\sqrt{R}} = \frac{-\frac{K_{12}}{\sqrt{K_{11} K_{22}}}}{\sqrt{\frac{K_{11}}{K_{22}}}} = \frac{-\frac{K_{12}}{\sqrt{K_{11} K_{22}}}}{\sqrt{\frac{K_{11}}{K_{22}}}} \frac{\sqrt{K_{22}}}{\sqrt{K_{22}}} = -K_{12}$$

$$\frac{\psi}{\sqrt{R}} = -K_{12}$$

c) $R = \frac{K_{11}}{K_{22}} = \frac{1}{K_{22}}$ since $K_{11} = 1$

$$K_{22} = \frac{1}{R}$$

2.

Figure 10. Supporting historical material showing the analysis context and documentation trail for the forward-swept-wing flutter investigation.

d) $M_{12} = -m x_\alpha \ell/2$

$M_{11} = m r_\alpha^2$

$s^2 = \frac{\bar{s}^2}{M_{11}} = \frac{\bar{s}^2}{m r_\alpha^2}$

$s^2 M_{12} = \left\{\frac{\bar{s}^2}{m r_\alpha^2}\right\}\left\{-m x_\alpha \ell/2\right\}$

$s^2 M_{12} = \bar{s}^2\left(-\frac{x_\alpha \ell}{2 r_\alpha^2}\right) = \bar{s}^2\left(\frac{-x_\alpha/c \;\; \ell/c}{2\, r_\alpha^2/c^2}\right)$

$s^2 M_{12} = \bar{s}^2\left(\frac{-\bar{x}_\alpha \; \ell/c}{2\bar{r}_\alpha^2}\right)$

$s^2 M_{12} = \bar{s}^2\left(\frac{-\bar{x}_\alpha \, \overline{AR}}{2\bar{r}_\alpha^2}\right)$ where : $\overline{AR} = \ell/c$, $\bar{x}_\alpha = \frac{x_\alpha}{c}$ and $\bar{r}_\alpha = r_\alpha/c$

e) $s^2 M_{22} = \frac{\bar{s}^2}{m r_\alpha^2}\,\frac{m \ell^2}{3} = \frac{\bar{s}^2 \ell^2}{3 r_\alpha^2}$

$s^2 M_{22} = \frac{\bar{s}^2 \ell^2/c^2}{3\, r_\alpha^2/c^2}$

$s^2 M_{22} = \frac{\bar{s}^2 \overline{AR}^2}{3\bar{r}_\alpha^2}$

f. $M_{11} = 1$

Summary of Substitution Variables For Stiffness/Mass Matrix

$s^2 M_{11} = \bar{s}^2$; $K_{11} = 1$; $s^2 M_{12} = \bar{s}^2\left(\frac{-\bar{x}_\alpha \overline{AR}}{2\bar{r}_\alpha^2}\right)$; $K_{12} = -\frac{\psi}{R}$

$K_{22} = \frac{1}{R}$; $s^2 M_{22} = \frac{\bar{s}^2 \overline{AR}^2}{3\bar{r}_\alpha^2}$

Substitution variables For Aerodynamic Matrix:

$[A] = q\, S\, C_{\ell_\alpha} \cos^2\Lambda \begin{bmatrix} -e & e\tan\Lambda \\ -y_{cp} & y_{cp}\tan\Lambda \end{bmatrix}$

$q = \frac{1}{2}\rho V^2$; $S = \ell c$ $\overline{AR} = \ell/c$

$[A] = \frac{1}{2}\rho V^2 (\ell c)\, C_{\ell_\alpha} \cos^2\Lambda \begin{bmatrix} -e & e\tan\Lambda \\ -y_{cp} & y_{cp}\tan\Lambda \end{bmatrix}$

$\bar{V} = \frac{V}{\omega_p c/2}$ and $\omega_p = \sqrt{\frac{K_{11}}{M_{11}}}$ and $K_{11} = 1 \Rightarrow \omega_p = \frac{1}{\sqrt{M_{11}}}$

$V = \omega_p \frac{c}{2}\bar{V}$

$V = \frac{1}{\sqrt{M_{11}}}\frac{c}{2}\bar{V}$

$V^2 = \left(\frac{c}{2}\right)^2 \frac{\bar{V}^2}{M_{11}}$; $M_{11} = m r_\alpha^2$

$V^2 = \frac{c^2 \bar{V}^2}{4 m r_\alpha^2} = \left(\frac{c}{2}\right)^2 \frac{\bar{V}^2}{m r_\alpha^2}$

$[A] = \frac{1}{2}\rho\left[\left(\frac{c}{2}\right)^2 \frac{\bar{V}^2}{m r_\alpha^2}\right] S\, C_{\ell_\alpha} \cos^2\Lambda \begin{bmatrix} -e & e\tan\Lambda \\ -y_{cp} & y_{cp}\tan\Lambda \end{bmatrix} \begin{Bmatrix} \bar{\theta} \\ \bar{\phi} \end{Bmatrix}$

$[A] = \frac{1}{2}\rho\left(\frac{c}{2}\right)\left(\frac{c}{2}\right)\frac{\bar{V}^2}{m r_\alpha^2}\, S\, C_{\ell_\alpha} \cos^2\Lambda \begin{bmatrix} -e & e\tan\Lambda \\ -y_{cp} & y_{cp}\tan\Lambda \end{bmatrix} \begin{Bmatrix} \bar{\theta} \\ \bar{\phi} \end{Bmatrix}$

$[A] = \frac{1}{2}(\bar{V}\cos\Lambda)^2 C_{\ell_\alpha} \frac{1}{\pi}\left\{\frac{\pi\rho\frac{c}{2}S}{2m}\right\}\frac{c}{r_\alpha^2}\,\frac{\frac{c}{2}}{c^2}\begin{bmatrix} -e & e\tan\Lambda \\ -y_{cp} & y_{cp}\tan\Lambda \end{bmatrix}\begin{Bmatrix} \bar{\theta} \\ \bar{\phi} \end{Bmatrix}$

assume: $\mu = \frac{2m}{\pi\rho\frac{c}{2}S}$

$[A] = \frac{1}{2}\frac{(\bar{V}\cos\Lambda)^2 C_{\ell_\alpha}}{\pi\mu\frac{r_\alpha^2}{c}}\frac{1}{c}\begin{bmatrix} -e & e\tan\Lambda \\ -y_{cp} & y_{cp}\tan\Lambda \end{bmatrix}\begin{Bmatrix} \bar{\theta} \\ \bar{\phi} \end{Bmatrix}$

$[A] = \frac{1}{2}\frac{(\bar{V}\cos\Lambda)^2}{\pi\mu\bar{r}_\alpha^2} C_{\ell_\alpha}\begin{bmatrix} -\frac{e}{c} & \frac{e}{c}\tan\Lambda \\ -\frac{y_{cp}}{\ell}\underbrace{\frac{\ell}{c}}_{\overline{AR}} & \frac{y_{cp}}{\ell}\underbrace{\frac{\ell}{c}}_{\overline{AR}}\tan\Lambda \end{bmatrix}\begin{Bmatrix} \bar{\theta} \\ \bar{\phi} \end{Bmatrix}$; $\ell/c = \overline{AR}$, $\frac{e}{c} = \bar{e}$, $\frac{y_{cp}}{\ell} = \bar{y}$

$[A] = \frac{1}{2}\frac{(\bar{V}\cos\Lambda)^2}{\pi\mu\bar{r}_\alpha^2} C_{\ell_\alpha}\begin{bmatrix} -\bar{e} & \bar{e}\tan\Lambda \\ -\bar{y}\,\overline{AR} & \bar{y}\,\overline{AR}\tan\Lambda \end{bmatrix}\begin{Bmatrix} \bar{\theta} \\ \bar{\phi} \end{Bmatrix}$

The above is the reduced form of the Aerodynamic Matrix:

The Equation of Motion Becomes:

$$\begin{bmatrix} (\bar{s}^2+1) & \left(\bar{s}^2\left[\frac{-\bar{x}_\alpha\overline{AR}}{2\bar{r}_\alpha^2}\right] - \frac{\psi}{\sqrt{R}}\right) \\ \left(\bar{s}^2\left[\frac{-\bar{x}_\alpha\overline{AR}}{2\bar{r}_\alpha^2}\right] - \frac{\psi}{\sqrt{R}}\right) & \left(\frac{\bar{s}^2\overline{AR}^2}{3\bar{r}_\alpha^2} + \frac{1}{R}\right) \end{bmatrix}\begin{Bmatrix} \bar{\theta} \\ \bar{\phi} \end{Bmatrix} + \frac{1}{2}\left(\frac{(\bar{V}\cos\Lambda)^2 C_{\ell_\alpha}}{\pi\mu\bar{r}_\alpha^2}\right)\begin{bmatrix} -\bar{e} & \bar{e}\tan\Lambda \\ -\bar{y}\,\overline{AR} & \bar{y}\,\overline{AR}\tan\Lambda \end{bmatrix}\begin{Bmatrix} \bar{\theta} \\ \bar{\phi} \end{Bmatrix} = \begin{Bmatrix} 0 \\ 0 \end{Bmatrix}$$

Equation 14

Figure 11. Archival material further documenting the computational basis and development history behind the corrected aeroelastic stability analysis.

$$\begin{bmatrix} (\bar{\xi}^2+1) & \left(\bar{\xi}^2\left[\frac{-\bar{x}_\alpha \bar{R}}{2\bar{r}_\alpha^2}\right]-\frac{\psi}{\sqrt{R}}\right) \\ \left(\bar{\xi}^2\left[\frac{-\bar{x}_\alpha \bar{R}}{2\bar{r}_\alpha^2}-\frac{\psi}{\sqrt{R}}\right)\left(\frac{\bar{\xi}^2\bar{R}^2}{3\bar{r}_\alpha^2}+\frac{1}{R}\right)\right. & \end{bmatrix}\begin{Bmatrix}\bar{\sigma}\\ \bar{\phi}\end{Bmatrix} + \frac{1}{2}\left(\frac{(\bar{V}\cos\Lambda)^2 C_{l_\alpha}}{\pi\mu\bar{r}_\alpha^2}\right)\begin{bmatrix}-\bar{e} & e\tan\Lambda \\ -\bar{y}\bar{R} & \bar{y}\bar{R}\tan\Lambda\end{bmatrix}\begin{Bmatrix}\bar{\sigma}\\ \bar{\phi}\end{Bmatrix} = \begin{Bmatrix}\phi\\ \phi\end{Bmatrix}$$

$$C_1 = -\frac{\bar{x}_\alpha \bar{R}}{2\bar{r}_\alpha^2}\ ,\quad C_2 = \frac{\psi}{\sqrt{R}}\ ,\quad C_3 = \frac{\bar{R}^2}{3\bar{r}_\alpha^2}\ ,\quad C_4 = \frac{1}{R}\ ,\quad C_5 = \frac{1}{2}\left(\frac{(\bar{V}\cos\Lambda)^2 C_{l_\alpha}}{\pi\mu\bar{r}_\alpha^2}\right)\ ,\quad C_6 = -\bar{e}$$

$$C_7 = \bar{e}\tan\Lambda\ ,\quad C_8 = -\bar{y}\bar{R}\ ,\quad C_9 = \bar{y}\bar{R}\tan\Lambda$$

$$\begin{bmatrix}(\bar{\xi}^2+1) & \bar{\xi}^2 C_1 - C_2 \\ \bar{\xi}^2 C_1 - C_2 & \bar{\xi}^2 C_3 + C_4\end{bmatrix}\begin{Bmatrix}\bar{\sigma}\\ \bar{\phi}\end{Bmatrix} + C_5\begin{bmatrix}C_6 & C_7 \\ C_8 & C_9\end{bmatrix}\begin{Bmatrix}\bar{\sigma}\\ \bar{\phi}\end{Bmatrix} = \begin{Bmatrix}0\\ 0\end{Bmatrix}$$

Frequency Form of The Equations:

$$\begin{bmatrix}(\bar{\xi}^2+1)+C_5C_6 & \bar{\xi}^2C_1-C_2+C_5C_7 \\ \bar{\xi}^2C_1-C_2+C_5C_8 & \bar{\xi}^2C_3+C_4+C_5C_9\end{bmatrix}\begin{Bmatrix}\bar{\sigma}\\ \bar{\phi}\end{Bmatrix} = \begin{Bmatrix}0\\ 0\end{Bmatrix}\ ;\quad [FM]\begin{Bmatrix}\bar{\sigma}\\ \phi\end{Bmatrix} = \begin{Bmatrix}0\\ 0\end{Bmatrix}$$

DET [Frequency Matrix] = 0

It has the following form:

$a\bar{\xi}^4 - b\bar{\xi}^2 - d\bar{V}_\alpha\bar{\xi}^2 + f + \bar{V}_\alpha g = 0$

Solve for a, b, d, f and g.

$$\overset{(a)}{\left[\bar{\xi}^2+1+C_5C_6\right]}\left[\bar{\xi}^2C_3+C_4+C_5C_9\right] - \overset{(b)}{\left[\bar{\xi}^2C_1-C_2+C_5C_8\right]}\left[\bar{\xi}^2C_1-C_2+C_5C_7\right] = 0$$

a)

$$\begin{array}{l} \bar{\xi}^2C_3+C_4+C_5C_9 \\ \times\ \underline{\bar{\xi}^2+1+C_5C_6} \\ \bar{\xi}^4C_3+\bar{\xi}^2C_4+\bar{\xi}^2C_5C_9 \\ \qquad\qquad +\bar{\xi}^2C_3+C_4+C_5C_9 \\ +\bar{\xi}^2C_3C_5C_6+C_4C_5C_6+C_5^2C_6C_9 \\ \hline \bar{\xi}^4C_3+\bar{\xi}^4C_4+\bar{\xi}^2C_5C_9+\bar{\xi}^2C_3+\bar{\xi}^2C_3C_5C_6+C_4C_5C_6+C_5^2C_6C_9+C_5C_9+C_4 \end{array}$$

b)

$$\begin{array}{l} \bar{\xi}^2C_1-C_2+C_5C_8 \\ \times\ \underline{\bar{\xi}^2C_1-C_2+C_5C_7} \\ \bar{\xi}^4C_1^2-\bar{\xi}^2C_1C_2+\bar{\xi}^2C_1C_5C_7 \\ \qquad\qquad -\bar{\xi}^2C_1C_2+C_2^2-C_2C_5C_8 \\ \underline{\bar{\xi}^2C_1C_5C_7-C_2C_5C_7+C_5^2C_7C_8} \\ \bar{\xi}^4C_1^2-\bar{\xi}^2C_1C_2+\bar{\xi}^2C_1C_5C_7-\bar{\xi}^2C_1C_2+\bar{\xi}^2C_1C_5C_7-C_2C_5C_7-C_2C_5C_8+C_5^2C_7C_8+C_2^2 \end{array}$$

Substituting:

$$\bar{\xi}^4C_3+\bar{\xi}^4C_4+\bar{\xi}^2C_5C_9+\bar{\xi}^4C_3+\bar{\xi}^2C_3C_5C_6+C_4C_5C_6+C_5^2C_6C_9+C_5C_9+C_4$$
$$-\bar{\xi}^4C_1^2+\bar{\xi}^2C_1C_2-\bar{\xi}^2C_1C_5C_7+\bar{\xi}^2C_1C_2-\bar{\xi}^2C_1C_5C_7+C_2C_5C_7+C_2C_5C_8-C_5^2C_7C_8-C_2^2=0$$

$$\bar{\xi}^4C_3-\bar{\xi}^4C_1^2+\left\{\bar{\xi}^2C_4+\bar{\xi}^2C_3+\bar{\xi}^2C_1C_2+\bar{\xi}^2C_1C_2\right\}+\left\{\bar{\xi}^2C_5C_9+\bar{\xi}^2C_3C_5C_6-\bar{\xi}^2C_1C_5C_7-\bar{\xi}^2C_1C_5C_8\right\}$$
$$+\left\{C_4+C_5C_9+C_5^2C_6C_9+C_4C_5C_6-C_5^2C_7C_8+C_2C_5C_8+C_2C_5C_7-C_2^2\right\}=0$$

$$\bar{\xi}^4\left\{C_3-C_1^2\right\}+\bar{\xi}\left\{C_4+C_3+2C_1C_2\right\}+\bar{\xi}^2\left\{C_5C_9+C_3C_5C_6-C_1C_5C_7-C_1C_5C_8\right\}$$
$$+\left\{C_5C_9+C_5^2C_6C_9+C_4C_5C_6-C_5^2C_7C_8+C_2C_5C_8+C_2C_5C_7\right\}$$
$$+\left\{C_4-C_2^2\right\}=0$$

4.

Figure 12. Additional historical evidence showing how the original computational work supported later verification of the corrected flutter and divergence equations.

$$s^4\left\{\frac{\overline{AR}^2}{3\bar{r}_\alpha^2}-\frac{\bar{X}_\alpha^2\overline{AR}^2}{(2\bar{r}_\alpha^2)^2}\right\}+s^2\left\{\frac{1}{R}+\frac{\overline{AR}^2}{3\bar{r}_\alpha^2}-\frac{\bar{X}_\alpha\overline{AR}}{\bar{r}_\alpha^2}\frac{\psi}{\sqrt{R}}\right\}+s^2\left\{\frac{1}{2}\frac{\bar{V}_n^2C_{L_\alpha}}{\pi\mu\bar{r}_\alpha^2}\bar{y}\,\overline{AR}\tan\Lambda+\frac{\overline{AR}^2}{3\bar{r}_\alpha^2}\frac{1}{2}\frac{\bar{V}_n^2C_{L_\alpha}}{\pi\mu\bar{r}_\alpha^2}(-\bar{e})-\left(\frac{-\bar{X}_\alpha\overline{AR}}{2\bar{r}_\alpha^2}\right)\frac{1}{2}\frac{\bar{V}_n^2C_{L_\alpha}}{\pi\mu\bar{r}_\alpha^2}\bar{e}\tan\Lambda-\frac{\bar{X}_\alpha\overline{AR}}{2\bar{r}_\alpha^2}\frac{1}{2}\frac{\bar{V}_n^2C_{L_\alpha}}{\pi\mu\bar{r}_\alpha^2}(\bar{y}\,\overline{AR})\right\}-\left\{\frac{1}{R}-\left(\frac{\psi}{\sqrt{R}}\right)^2\right\}$$

see NOTE #1

$$s^4\frac{\overline{AR}^2}{3\bar{r}_\alpha^2}\left\{\frac{\bar{r}_\alpha^2+\frac{1}{4}\bar{X}_\alpha^2}{\bar{r}_\alpha^2}\right\}+s^2\frac{1}{R}\left\{1+\frac{R\overline{AR}^2}{3\bar{r}_\alpha^2}-\frac{\bar{X}_\alpha R\overline{AR}\psi}{\bar{r}_\alpha^2\sqrt{R}}\right\}+\bar{V}_n^2s^2\left(\frac{C_{L_\alpha}}{2\pi\mu\bar{r}_\alpha^2}\right)\overline{AR}\left\{\bar{y}\tan\Lambda-\frac{\overline{AR}}{3\bar{r}_\alpha^2}\bar{e}+\frac{\bar{X}_\alpha}{2\bar{r}_\alpha^2}\bar{e}\tan\Lambda-\frac{\bar{X}_\alpha}{2\bar{r}_\alpha^2}\bar{y}\,\overline{AR}\right\}$$

(a)

see NOTE #2

$$s^2\frac{1}{R}\left\{1+\frac{R\overline{AR}^2}{3\bar{r}_\alpha^2}-\frac{\bar{X}_\alpha\overline{AR}\sqrt{R}\psi}{\bar{r}_\alpha^2}\right\}+\bar{V}_n^2s^2\left(\frac{C_{L_\alpha}}{2\pi\mu\bar{r}_\alpha^2}\right)\overline{AR}\left\{\bar{y}\tan\Lambda-\frac{\overline{AR}}{3\bar{r}_\alpha^2}\bar{e}+\frac{\bar{X}_\alpha}{2\bar{r}_\alpha^2}(\bar{e}\tan\Lambda-\bar{y}\,\overline{AR})\right\}$$

(b) (d)

see NOTE #3

$\mathcal{E}$

$$+\left(\frac{1}{2}\frac{\bar{V}_n^2C_{L_\alpha}}{\pi\mu\bar{r}_\alpha^2}\right)\bar{y}\,AR\tan\Lambda-\cancel{\left(\frac{1}{2}\frac{\bar{V}_n^2C_{L_\alpha}}{\pi\mu\bar{r}_\alpha^2}\right)^2\bar{e}\,y\,AR\tan\Lambda}-\frac{1}{R}\left(\frac{1}{2}\frac{\bar{V}_n^2C_{L_\alpha}}{\pi\mu\bar{r}_\alpha^2}\right)\bar{e}+\cancel{\left(\frac{1}{2}\frac{\bar{V}_n^2C_{L_\alpha}}{\pi\mu\bar{r}_\alpha^2}\right)^2\bar{e}\tan\Lambda\,y\,AR}-\frac{\psi}{\sqrt{R}}\left(\frac{1}{2}\frac{\bar{V}_n^2C_{L_\alpha}}{\pi\mu\bar{r}_\alpha^2}\right)y\,AR+\frac{\psi}{\sqrt{R}}\left(\frac{1}{2}\frac{\bar{V}_n^2C_{L_\alpha}}{\pi\mu\bar{r}_\alpha^2}\right)\bar{e}\tan\Lambda$$

$$\left(\frac{1}{2}\frac{\bar{V}_n^2C_{L_\alpha}}{\pi\mu\bar{r}_\alpha^2}\right)\bar{y}\,\overline{AR}\tan\Lambda-\frac{1}{R}\left(\frac{1}{2}\frac{\bar{V}_n^2C_{L_\alpha}}{\pi\mu\bar{r}_\alpha^2}\right)\bar{e}-\frac{\psi}{\sqrt{R}}\left(\frac{1}{2}\frac{\bar{V}_n^2C_{L_\alpha}}{\pi\mu\bar{r}_\alpha^2}\right)\bar{y}\,\overline{AR}+\frac{\psi}{\sqrt{R}}\left(\frac{1}{2}\frac{\bar{V}_n^2C_{L_\alpha}}{\pi\mu\bar{r}_\alpha^2}\right)\bar{e}\tan\Lambda$$

$$\bar{V}_n^2\cdot\frac{C_{L_\alpha}}{2\pi\mu\bar{r}_\alpha^2}\left\{\bar{y}\,\overline{AR}\tan\Lambda-\frac{1}{R}\bar{e}+\frac{\psi}{\sqrt{R}}(\bar{e}\tan\Lambda-\bar{y}\,\overline{AR})\right\}$$

$$\bar{V}_n^2\cdot\frac{C_{L_\alpha}}{2\pi\mu\bar{r}_\alpha^2}\left\{-\frac{1}{R}\bar{e}+\bar{y}\,\overline{AR}\tan\Lambda+\frac{\psi}{\sqrt{R}}(\bar{e}\tan\Lambda-\bar{y}\,\overline{AR})\right\}$$

$$\bar{V}_n^2\cdot\frac{C_{L_\alpha}}{2\pi\mu\bar{r}_\alpha^2}\left\{\frac{1}{R}\left[-\bar{e}+R\,\bar{y}\,\overline{AR}\tan\Lambda+\psi\frac{R}{\sqrt{R}}(\bar{e}\tan\Lambda-\bar{y}\,\overline{AR})\right]\right\}$$

$$\bar{V}_n^2\cdot\frac{C_{L_\alpha}}{2\pi\mu\bar{r}_\alpha^2}\left\{\frac{1}{R}\left[-\bar{e}+R\,\bar{y}\,\overline{AR}\tan\Lambda+\psi\sqrt{R}(\bar{e}\tan\Lambda-\bar{y}\,\overline{AR})\right]\right\}$$

$$\bar{V}_n^2\,\mathcal{E}\left\{\frac{1}{R}\left[-\bar{e}+R\,\bar{y}\,\overline{AR}\tan\Lambda+\psi\sqrt{R}(\bar{e}\tan\Lambda-\bar{y}\,\overline{AR})\right]\right\}+\frac{1}{R}-\left(\frac{\psi}{\sqrt{R}}\right)^2$$

(g)

$$\frac{1}{R}-\frac{\psi^2}{R}$$

$$(1-\psi^2)/R=0$$

using $as^4-bs^2-d\bar{V}_n^2s^2+\bar{V}_n^2g+f=0$ the coefficients are given as:

$$a=\frac{\overline{AR}^2}{3\bar{r}_\alpha^2}\left\{\frac{\bar{r}_\alpha^2+\frac{1}{4}\bar{X}_\alpha^2}{\bar{r}_\alpha^2}\right\}$$

$$b=-\frac{1}{R}\left\{1+\frac{R\overline{AR}^2}{3\bar{r}_\alpha^2}-\frac{\bar{X}_\alpha\overline{AR}\sqrt{R}\psi}{\bar{r}_\alpha^2}\right\}$$

$$d=-\mathcal{E}\,\overline{AR}\left\{\bar{y}\tan\Lambda-\frac{\overline{AR}}{3\bar{r}_\alpha^2}\bar{e}+\frac{\bar{X}_\alpha}{2\bar{r}_\alpha^2}(\bar{e}\tan\Lambda-\bar{y}\,\overline{AR})\right\}$$

$$g=\mathcal{E}\left\{\frac{1}{R}\left[-\bar{e}+R\,\bar{y}\,\overline{AR}\tan\Lambda+\psi\sqrt{R}(\bar{e}\tan\Lambda-\bar{y}\,\overline{AR})\right]\right\}$$

$$f=(1-\psi^2)/R \quad \text{and} \quad \mathcal{E}=\frac{C_{L_\alpha}}{2\pi\mu\bar{r}_\alpha^2}$$

NOTE #1:

$$\frac{\overline{AR}^2}{3\bar{r}_\alpha^2}-\frac{\bar{X}_\alpha^2\overline{AR}^2}{(2\bar{r}_\alpha^2)^2}=\frac{\overline{AR}^2}{3\bar{r}_\alpha^2}-\frac{3\bar{X}_\alpha^2\overline{AR}^2}{3(2\bar{r}_\alpha^2)^2}=\frac{\overline{AR}^2}{3\bar{r}_\alpha^2}\left(1-\frac{3\bar{X}_\alpha^2}{(2)^2\bar{r}_\alpha^2}\right);\quad \bar{r}_\alpha^2=\bar{r}_0^2+\bar{X}_\alpha^2$$

$$=\frac{\overline{AR}^2}{3\bar{r}_\alpha^2}\left(\frac{4\bar{r}_\alpha^2}{4\bar{r}_\alpha^2}-\frac{3\bar{X}_\alpha^2}{4\bar{r}_\alpha^2}\right)=\frac{\overline{AR}^2}{3\bar{r}_\alpha^2}\left(\frac{4\bar{r}_\alpha^2-3\bar{X}_\alpha^2}{4\bar{r}_\alpha^2}\right)=\frac{\overline{AR}^2}{3\bar{r}_\alpha^2}\left(\frac{4(\bar{r}_0^2+\bar{X}_\alpha^2)-3\bar{X}_\alpha^2}{4\bar{r}_\alpha^2}\right)$$

$$=\frac{\overline{AR}^2}{3\bar{r}_\alpha^2}\left(\frac{4\bar{r}_0^2+4\bar{X}_\alpha^2-3\bar{X}_\alpha^2}{4\bar{r}_\alpha^2}\right)=\frac{\overline{AR}^2}{3\bar{r}_\alpha^2}\left(\frac{4\bar{r}_0^2+\bar{X}_\alpha^2}{4\bar{r}_\alpha^2}\right)$$

$$=\frac{\overline{AR}^2}{3\bar{r}_\alpha^2}\left(\frac{\bar{r}_0^2+\frac{1}{4}\bar{X}_\alpha^2}{\bar{r}_\alpha^2}\right)$$

NOTE #2:

$$\frac{R}{\sqrt{R}}=\frac{R}{\sqrt{R}}\frac{\sqrt{R}}{\sqrt{R}}=\frac{R\sqrt{R}}{R}=\sqrt{R}$$

$$\frac{R}{\sqrt{R}}=\sqrt{R}$$

NOTE #3:

$$\mathcal{E}=\frac{C_{L_\alpha}}{2\pi\mu\bar{r}_\alpha^2}$$

5a

Figure 13. Historical documentation connecting the stiffness cross-coupling analysis to the author's broader aeroelastic and flutter-compatibility work.

Compute the Flutter Velocity From the previous derivation:

$\bar{s} = j\Omega$ where $\Omega = \omega/\omega_p$

eqn (19) becomes:

$a\Omega^4 + (b + \bar{V}_n^2 d)\Omega^2 + (f + \bar{V}_n^2 g) = 0$; solving for Ω.

$\Omega^2 = \{-(b + \bar{V}_n^2 d \pm [(b + \bar{V}_n^2 d)^2 - 4a(f + \bar{V}_n^2 g)]^{1/2}\}/2a$ (See Derivation) $\longrightarrow$

The on-set of Flutter occurs when the expression under the radical is zero.

$(b + \bar{V}_n^2 d)^2 = 4a(f + \bar{V}_n^2 g)$

Solve for V_F

$b^2 + 2bd\bar{V}_n^2 + (\bar{V}_n^2)^2 d^2 = 4af + 4ag\bar{V}_n^2$

$d^2(\bar{V}_n^2)^2 + 2bd\bar{V}_n^2 - 4ag\bar{V}_n^2 + (b^2 - 4af) = 0$

$d^2(\bar{V}_n^2)^2 + (2bd - 4ag)\bar{V}_n^2 + (b^2 - 4af) = 0$

$d^2(\bar{V}_n^2)^2 + 2(bd - 2ag)\bar{V}_n^2 + (b^2 - 4af) = 0$

$\bar{V}_n = \bar{V}\cos\Lambda$

$a = d^2, \quad b = 2(bd - 2ag), \quad c = b^2 - 4af$

$$\bar{V}_n^2 = \frac{-2(bd - 2ag) \pm \sqrt{[2(bd - 2ag)]^2 - 4d^2(b^2 - 4af)}}{2d^2}$$

$$\bar{V}_n^2 = \frac{-2(bd - 2ag) \pm \sqrt{4(b^2d^2 - 4abdg + 4a^2g^2) - 4d^2b^2 + 16ad^2f}}{2d^2}$$

$$\bar{V}_n^2 = \frac{-2(bd - 2ag) \pm \sqrt{4b^2d^2 - 16abdg + 16a^2g^2 - 4d^2b^2 + 16ad^2f}}{2d^2}$$

$$\bar{V}_n^2 = \frac{-2(bd - 2ag) \pm \sqrt{16a[-bdg + ag^2 + d^2f]}}{2d^2}$$

$$\bar{V}_n^2 = \frac{-2(bd - 2ag) \pm 4\sqrt{a[-bdg + ag^2 + d^2f]}}{2d^2}$$

$$\bar{V}_n^2 = \frac{-(bd - 2ag) \pm 2[a(-bdg + ag^2 + d^2f)]^{1/2}}{d^2}$$

$$\bar{V}_F^2 = \frac{-(bd - 2ag) \pm 2[a(-bdg + ag^2 + d^2f)]^{1/2}}{d^2\cos^2\Lambda}$$

For purely Sinusoidal Motion:

$a\bar{s}^4 - b\bar{s}^2 - d\bar{V}_n^2\bar{s}^2 + f + \bar{V}_n^2 g = 0$

$\bar{s} = j\Omega$

$\bar{s}^2 = (j\Omega)(j\Omega) = -\Omega^2$

$\bar{s}^4 = \Omega^4$

$a\Omega^4 + b\Omega^2 + d\bar{V}_n^2\Omega^2 + f + \bar{V}_n^2 g = 0$

$a\Omega^4 + (b + d\bar{V}_n^2)\Omega^2 + (f\bar{V}_n^2 g) = 0$

$a(\Omega^2)^2 + (b + d\bar{V}_n^2)(\Omega^2) + (f + \bar{V}_n^2 g) = 0$

$$\Omega^2 = \frac{-(b + d\bar{V}_n^2) \pm \sqrt{(b + d\bar{V}_n^2) - 4a(f + \bar{V}_n^2 g)}}{2a}$$

Determinant of Stiffness Matrix:

$$[K] = \begin{bmatrix} K_{11} & K_{12} \\ K_{21} & K_{22} \end{bmatrix}$$

$\Delta = K_{11}K_{22} - K_{21}K_{12} \qquad K_{12} = K_{21}$

$\Delta = K_{11}K_{22} - K_{12}^2$

$\Delta = K_{11}K_{22}\left[1 - \frac{K_{12}^2}{K_{11}K_{22}}\right]$

since Stiffness Matrix must be positive definite:

$$\frac{K_{12}^2}{K_{11}K_{22}} < 1$$

Stiffness Cross-Coupling parameter is:

$$\psi = \frac{-K_{12}}{\sqrt{K_{11}K_{22}}}, \quad -1 < \psi < 1$$

6.

Figure 14. Final archival figure supporting the paper's historical note and showing the continuity between the original analysis effort and the corrected results presented here.

References

[1]Weisshaar, Ryan, *Control of Aeroelastic Instabilities Through Stiffness Cross-Coupling*, AIAA J. of Aircraft, 1986

[2]Bisplinghoff, Ashley, Halfman, *Aeroelasticity*, (Dover Publications, Inc. New York, 1996)

[3]Bernard Etkin, *Dynamics of Atmospheric Flight*, (Dover Publications, Inc. New York, 2005)

[4]John D. Anderson, *Computational Fluid Dynamics*, (McGraw-Hill, New York, 1995)

[5]John D. Anderson, *Introduction to Flight*, (McGraw-Hill, New York, 1989)

[6]John D. Anderson, *Fundamentals of Aerodynamics*, (McGraw-Hill, New York, 1984)

[7]Richard Von Mises, *Theory of Wing Sections*, (Dover Publications, Inc. New York, 1959)

[8]Richard Von Mises, *Theory of Flight*, (Dover Publications, Inc. New York, 1958)

Copyright © 2026 John Cipolla/AeroCFD.com